

Mutation of *SLC9A1*, encoding the major Na^+/H^+ exchanger, causes ataxia–deafness Lichtenstein–Knorr syndrome

Claire Guissart^{1,2,3}, Xiuju Li⁴, Bruno Leheup^{5,6}, Nathalie Drouot⁷, Bettina Montaut-Verient⁸, Emmanuel Raffo^{6,9}, Philippe Jonveaux^{6,10}, Anne-Françoise Roux^{1,3}, Mireille Claustres^{1,2,3}, Larry Fliegel⁴ and Michel Koenig^{1,2,3,7,*}

¹INSERM U827, Montpellier F-34000, France, ²Université Montpellier I, Montpellier F-34000, France, ³Laboratoire de Génétique Moléculaire, Centre Hospitalier Universitaire (CHU) Montpellier, Montpellier F-34000, France, ⁴Department of Biochemistry, Faculty of Medicine, University of Alberta, Edmonton, AB, Canada, ⁵Service de Médecine Infantile et Génétique Clinique, Centre de Référence Syndrome Malformatif et Anomalies du Développement, CHU de Nancy Pôle Enfants, 54511 Vandoeuvre cedex, France, ⁶INSERM U954, Faculté de Médecine, Université de Lorraine, 54505 Vandoeuvre cedex, France, ⁷Institut de Génétique et de Biologie Moléculaire et Cellulaire (IGBMC), INSERM U964/CNRS UMR7104/Université de Strasbourg, Illkirch, France, ⁸Service d'Oto-Rhino-Laryngologie et de Chirurgie Cervico-Faciale, CHU de Nancy, Vandoeuvre, France, ⁹Service de Neuropédiatrie, CHU de Nancy Pôle Enfants, 54511 Vandoeuvre cedex, France and ¹⁰Laboratoire de Génétique Médicale, CHU Nancy, INSERM U954, Université de Lorraine, Vandoeuvre, France

Received July 23, 2014; Revised and Accepted September 4, 2014

Lichtenstein–Knorr syndrome is an autosomal recessive condition that associates sensorineural hearing loss and cerebellar ataxia. Here, we report the first identification of a gene involved in Lichtenstein–Knorr syndrome. By using a combination of homozygosity mapping and whole-exome sequencing, we identified the homozygous p.Gly305Arg missense mutation in *SLC9A1* that segregates with the disease in a large consanguineous family. Mutant glycine 305 is a highly conserved amino acid present in the eighth transmembrane segment of all meta-zoan orthologues of NHE1, the Na^+/H^+ exchanger 1, encoded by *SLC9A1*. We demonstrate that the p.Gly305Arg mutation causes the near complete de-glycosylation, mis-targeting and loss of proton pumping activity of NHE1. The comparison of our family with the phenotypes of spontaneous and knockout *Slc9a1* murine models demonstrates that the association between ataxia and hearing loss is caused by complete or near complete loss of function of NHE1 and altered regulation of pH_i in the central nervous system.

INTRODUCTION

Autosomal recessive cerebellar ataxias are a heterogeneous group of inherited neurodegenerative disorders that affect the cerebellum, the spinocerebellar and sensory tracts of the spinal cord and often the sensory nerves. Recessive ataxias may present as a pure cerebellar syndrome or are associated with neurological symptoms such as peripheral neuropathy, dystonia, chorea, cognitive impairment, optic atrophy, seizures or extra neurological symptoms such as cardiomyopathy and diabetes

mellitus in Friedreich ataxia [MIM# 229300; (1)]. The main clinical features are staggering gait with frequent falls, upper limb dysmetria, impairment of speech, dysphagia and saccadic ocular pursuit.

The association of recessive ataxia with hypoacusia or deafness is uncommon. Ataxia and sensorineural hearing loss are seen in the pleiotropic syndromes PHARC (polyneuropathy, hearing loss, ataxia, retinitis pigmentosa and cataract) and Refsum disease, which also associate peripheral neuropathy, retinitis pigmentosa and ichthyosis (Refsum) or cataract (PHARC).

*To whom correspondence should be addressed at: INSERM, UMR_S 827, Institut Universitaire de Recherche Clinique, 641 Avenue du Doyen Gaston Giraud, 34093 Montpellier cedex5, France. Tel: +33 411 759 879; Fax: +33 411 759 882; Email: michel.koenig@inserm.fr

Refsum disease is caused by mutations in phytanoyl-CoA hydroxylase (*PHYH*) and peroxin 7 (*PEX7*), and PHARC is caused by mutations in alpha/beta hydroxylase 12 (*ABHD12*) (2). Hearing loss is a rare feature of Friedreich ataxia (seen in 7–13% of the cases) (3) and mitochondrial recessive ataxia syndrome (MIRAS) (4). The co-occurrence of ataxia and deafness of autosomal recessive origin has been described in a few syndromes, including Lichtenstein–Knorr syndrome (5–7) and Pratap-Chand syndrome (8). Pratap-Chand syndrome is an infantile form of olivopontocerebellar atrophy, failure to thrive, microcephaly and deafness reported in 11 families of Omani origin. Lichtenstein–Knorr syndrome is a juvenile/adolescent onset form of ataxia and sensorineural hearing loss, described for the first time in 1930 by Lichtenstein and Knorr (9). No gene has been identified as the cause of Pratap-Chand and Lichtenstein–Knorr syndromes.

We report here the identification, by whole-exome sequencing combined with homozygosity mapping analysis, of a homozygous missense mutation in the Na⁺/H⁺ exchanger isoform 1 [NHE1, encoded by *SLC9A1* (MIM 107310)] of a consanguineous family with Lichtenstein–Knorr syndrome. The causative involvement of the mutation, which introduces a positive charge in the middle of the eighth transmembrane segment of NHE1, was investigated by activity, expression and targeting analyses of the mutant protein. Functional disruption of NHE1 in the ataxia/deafness family and comparison with phenotypes of spontaneous and knockout murine models (10) demonstrate that isolated ataxia and hearing loss is caused by complete or near complete loss of function of NHE1 and altered regulation of pH_i in the central nervous system (CNS).

RESULTS

Three siblings born from first-degree consanguineous parents of Turkish origin were affected by early onset cerebellar ataxia and deafness (family C.). Clinical features are summarized in Table 1. All three siblings had normal birth and normal initial development but experienced delayed walking at ages ranging from 18 months to 5 years with aid required. From there on, they developed gait and limb ataxia. On clinical examination, the patients presented with cerebellar ataxia, dysmetria and adiadochokinesia. They also all had lower and upper limb areflexia, suggesting peripheral neuropathy. The two sisters had reduced sensory evoked potentials and normal motor conduction velocities (peripheral sensory nerve conduction was not recorded). Severe to profound sensorineural deafness was diagnosed at ages ranging from 12 to 20 months. The two girls had profound deafness with the lack of language and the lack of response at 100 dB on auditory evoked stimulation (Fig. 1). Vestibular investigation by caloric testing with hot water could only be performed with the younger sister for the right ear and revealed hyporeflexia. The younger boy had severe deafness with the lack of V wave at 110 dB stimulation (Fig. 1). He learned hand sign language. The two girls had café-au-lait spots on the left thigh. Lactate and pyruvate measurements, performed in order to test for a mitochondrial disorder, were normal. Cerebral magnetic resonance imaging (MRI) was normal in the older girl and revealed very mild vermian atrophy in the younger girl (Fig. 1). At the age of 14 years, the younger sister was

Table 1. Clinical and neurophysiological findings of the three patients of family C.

Patient	II.1	II.2	II.3
Present age (years)	22	21	17
Gender	F	F	M
Deafness	Profound	Profound	Severe
Age at diagnosis of deafness (months)	20	16	12
Auditory evoked potentials	Lack of response at 100 dB	Lack of response at 100 dB	Lack of V wave at 110 dB
Language	None	None	Sign language
Vestibular system	Not tested	Hyporeflexia	Not tested
Ocular system	Normal	Normal	Normal
Delayed walking	Until 2 years	Until 18 months	Until 5 years, with aid
Ataxia	Present since walking	Present since walking	Present since 3 years
Deep tendon reflexes	Areflexia	Areflexia	Areflexia
Motor conduction velocity	Normal	Normal	Not done
Sensory evoked potentials	Decreased	Decreased	Not done
Cerebral MRI	Normal	Mild vermian atrophy	Not done
Electroencephalogram	Not done	Normal at 14 years	Not done
Muscle biopsy	Not done	Normal	Not done
Stature	Normal	Normal	–3 SD at 16 years
Puberty	Normal	Normal	Delayed
Café-au-lait spots	On left thigh	On left thigh	None
Lactate/pyruvate ratio	Normal	Normal	Normal

hospitalized following a malaise with clonic jerks evoking seizure. Two electroencephalograms (EEGs) performed on this occasion were normal. The boy had delayed puberty with normal luteinizing-hormone–releasing hormone response and a short stature at age 16 years [–3.7 standard deviation (SD)].

Because of consanguinity of the parents, homozygosity mapping was performed by whole-genome single-nucleotide polymorphism (SNP) analysis of the patients. SNP analysis revealed two significant regions of homozygosity shared by the three affected siblings, one on chromosome 1 (23.6 Mb; 294 consecutive homozygous SNPs between rs725389 and rs841851), and one on chromosome 7 (5.5 Mb; 57 consecutive homozygous SNPs between rs6464907 and rs3899133; Fig. 2A). Since exome sequencing of patient IV.1 revealed no mutation in known ataxia or deafness genes, variants located in the two regions of shared homozygosity were investigated. Seven homozygous variations with a frequency of <1% in dbSNP 137 were found in the region on chromosome 1 and none were identified in the region on chromosome 7.

Of the seven variants located in the shared homozygous regions, two were intronic and one was located in a 3' untranslated region (UTR) region. All the three variants had frequency ranging from 0.5 to 0.8% in dbSNP137 and were referenced in the Ensembl SNP database (rs115769731, rs11586791 and rs141375854). None of the intronic and 3'UTR variants were likely pathogenic since they were not predicted by the Human Splicing Finder (HSF) (11) to affect adjacent splice sites or to activate cryptic splice sites.

The four remaining variants were located in exon coding sequences, two of which had frequency of 0.5 and 0.6% in

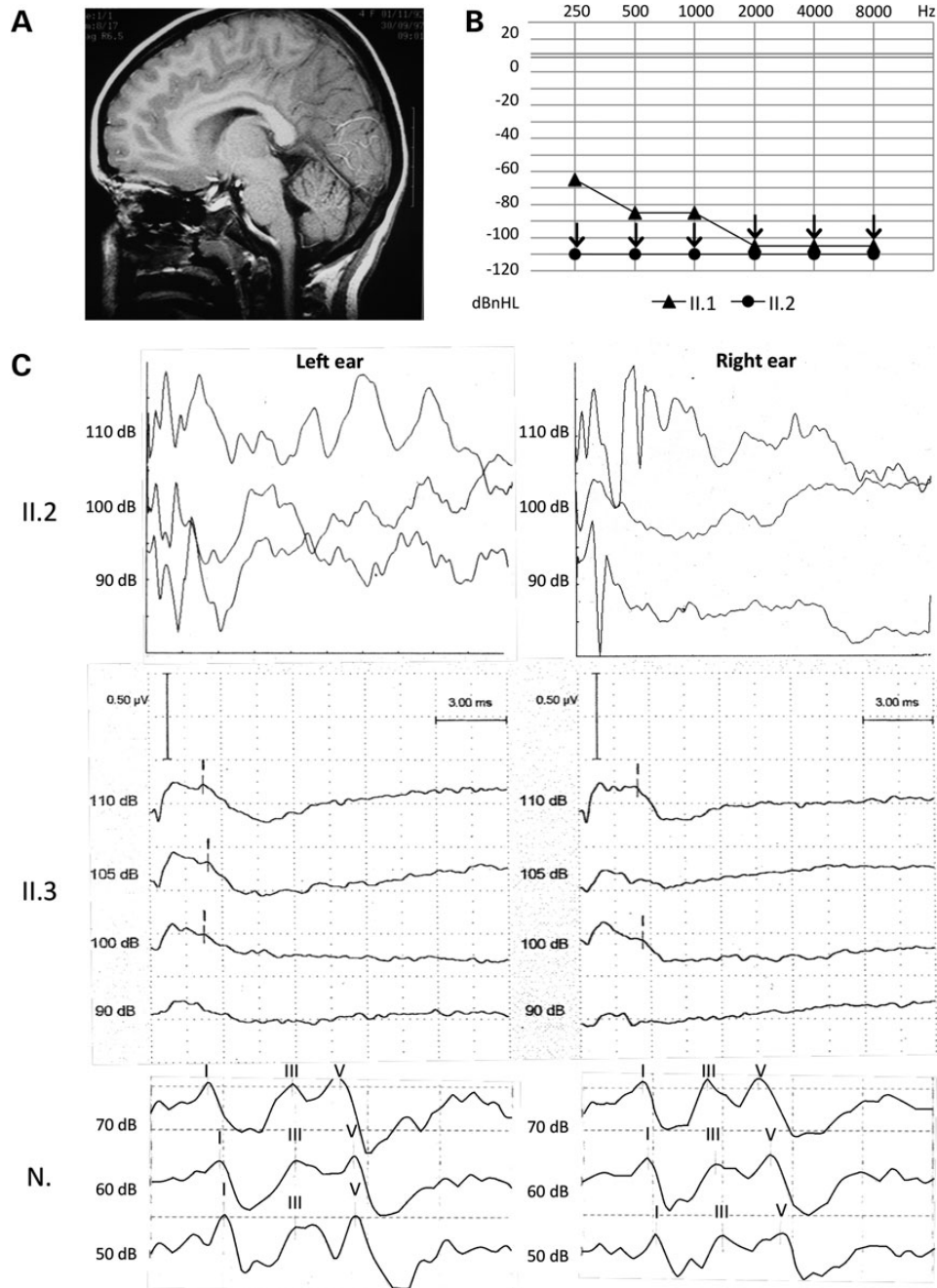


Figure 1. MRI and auditory findings in patients of family C. (A) MRI of patient II.2 reveals very mild anterior vermian atrophy at 5 years of age. (B) Pure tone audiograms (PTAs) of the sisters. PTAs recorded, respectively, at 6 (II.1) and 8 years of age (II.2) show profound hearing loss for both sisters (no perception at -110 dB from 2000 to 8000 Hz). Arrows indicate no sound was perceived. (C) Auditory brainstem responses (ABRs) of patients II.2, II.3 and normal individual (N.). The recording of ABRs of patient II.2 (recorded at 29 months) shows anarchic traces and no individualized wave up to a stimulation intensity of 110 dB on both ears. The recording of ABRs of patient II.3 (at age 17 months) reveals the absence of V wave up to a stimulation intensity of 110 dB on both ears. ABR recording of a normal individual shows individualized waves I, III and V on both ears at a stimulation intensity of 70 dB and lower.

dbSNP137 and were referenced in the Ensembl SNP database. One was a synonymous variant located at position +1 of the acceptor splice site of the seventh exon of the *CATSPER4* gene (c.813G>A, p.Gln271Gln; rs144835190). This variant was not predicted pathogenic by HSF (score: -0.29%). One other variant was a missense change located in the *SDC3* gene (c.286G>A, p.Ala96Thr, rs41269523). This change was predicted deleterious by SIFT (score: 0.02). However, it was

predicted neutral by Polyphen2 and had a minor allele frequency $>1\%$ in the European American population (Exome Sequencing Project, EVS database). One of the two novel variants was a synonymous variant located in the *HSPG2* gene (c.11628C>T, p.Thr3876Thr). It was not predicted by *in silico* analyses to activate a cryptic splice site.

The only other novel variant in the shared regions of homozygosity (position chr1: 27436169 C>T [hg19], 76 reads

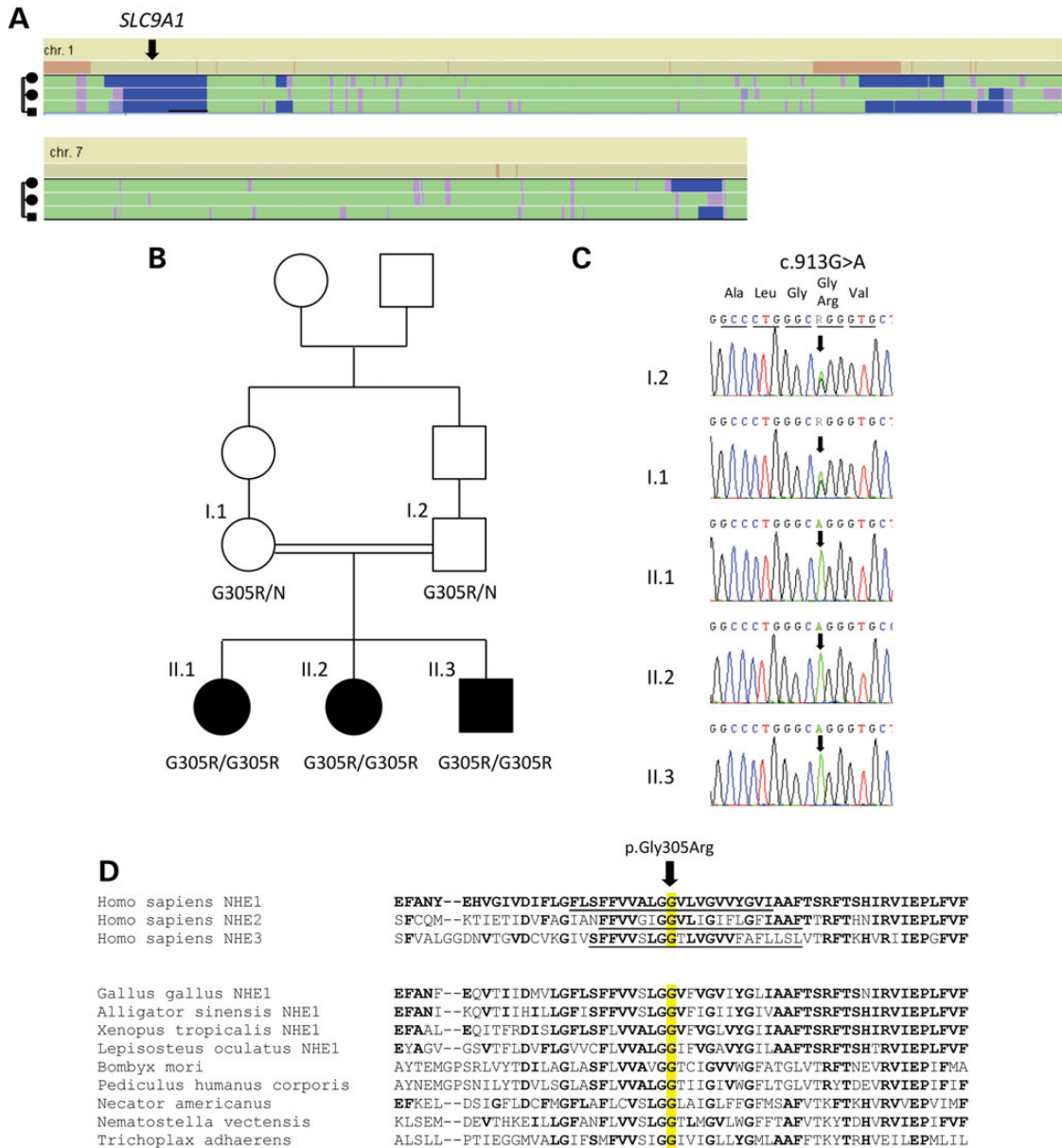


Figure 2. Identification of NHE1 mutation in family C. (A) Whole-genome homozygosity mapping results. SNP genotyping results of the three affected children were analyzed with the HomoSNP software (<http://bips.u-strasbg.fr/HomoSNP/>) to map homozygous regions across the 22 autosomes. Results are shown for chromosomes 1 and 7, which were the only chromosomes that revealed significant regions of homozygosity shared among the three affected children. Each colored lane represents one patient; the pedigree is indicated on the left of each chromosome. Homozygous regions are colored according to the number of consecutive homozygous SNP markers: pink, from 35 to 39 markers; purple, from 40 to 45 markers; blue, more than 45 markers. Known loci for genes involved in ataxia are indicated in the line above the mapping results. The localization of *SLC9A1* on the homozygosity map of chromosome 1 is indicated by an arrow. (B) Pedigree showing consanguinity and segregation of the disease with mutation c.913G>A causing the p.Gly305Arg missense change (G305R). (C) Sanger sequencing of the mutation c.913G>A: the three patients are homozygous for the substitution and the parents are heterozygous for the same substitution. (D) Sequence comparison of amino acids in the eighth transmembrane domain (underlined) of the human plasma membrane NHE proteins and of orthologous proteins from different species. Amino acids that are identical to the human NHE1 sequence are shown in bold. The missense mutation (on the top of the mutated amino acid glycine, G, highlighted in yellow) is indicated by an arrow. The mutated amino acid is conserved in all metazoan species.

coverage) was located in the *SLC9A1* gene (c.913G>A, exon 3), and is predicted to cause a non-conservative missense change of glycine 305 into arginine (p.Gly305Arg, Fig. 2B and C). *SLC9A1* encodes for NHE1 (Na⁺/H⁺ exchanger family member 1), a protein with 12 transmembrane helices. Glycine 305 is located in the eighth transmembrane segment of NHE1 and is a residue highly conserved through evolution (conserved in all

investigated metazoans, Fig. 2D). The replacement of glycine 305 (a small neutral amino acid in the transmembrane segment) by arginine, a positively charged amino acid, is predicted to be very probably pathogenic according to the Sift and Polyphen2 prediction programs (SIFT score: 0.01).

Sanger sequencing confirmed that the c.913G>A variant segregates with the disease (homozygous in all three patients

and heterozygous in the two parents; Fig. 2B and C). The c.913G>A/p.Gly305Arg variant therefore appears to be the causative mutation in family C.; this conclusion is further supported by the two independent *Slc9a1* mice models which present with a neurological syndrome that includes ataxia (10,12).

After identification and characterization of the mutation in family C., 172 patients with ataxia and/or hearing loss were analyzed by sequencing of the 12 coding exons of *SLC9A1*. We identified two missense and two synonymous heterozygous variants in patients with ataxia only. Both synonymous variants were referenced in the Ensembl SNP database with a frequency of 0.37 (c.1356C>T, p.Ile452 = rs35607809) and 0.0078% (c.1275C>T, p.Arg425 = rs370187243). Both missense variants were found in exon 12 and were predicted damaging by SIFT: c.2323G>C, p.Asp775His (SIFT score = 0.01) and c.2426C>T, p.Pro809Leu, rs144794319 (SIFT score = 0.00). However, none of the four variants appears to be disease causing since they are heterozygous in four distinct patients.

To conclusively demonstrate the pathogenicity of the p.Gly305Arg (G305R) change, we mutated cDNA for the NHE1 protein to create this mutation. The mutant protein was then stably expressed in AP-1 cells are a Chinese hamster ovary cell line that lack their own NHE1 protein. The NHE1 protein contains a hemagglutinin (HA) tag for detection. We have earlier determined that this tag does not affect NHE1 function (13). Initially, we examined the expression of the G305R mutant in AP-1 cells using western blot analysis (Fig. 3A). Cells stably transfected with wild-type (WT) NHE1 displayed the characteristic pattern of a 105–100 kDa immunoreactive protein and a second smaller protein of 80–90 kDa. This likely reflects different levels of glycosylation of the NHE1 protein (13). AP-1 cells, not transfected with NHE1, showed no such immunoreactive pattern. Cells transfected with the G305R mutant DNA also showed the presence of NHE1 protein, though this was entirely found as the lower molecular weight form. The amount of protein expressed was reduced. Quantification of the amount of NHE1 protein showed that it was reduced by about one-third (to $33.8 \pm 3.2\%$ of control levels).

We previously made mutations of the NHE1 protein to study its structure and function (13,14). Some of these resulted in protein mis-targeting, with a reduced amount of NHE1 protein on the cell surface. To determine if the G305R mutation resulted in aberrant targeting of the NHE1 protein to the cell surface, we initially examined cell surface targeting of the mutant protein in comparison with the WT using a quantitative approach with cell surface labeling by sulfo-NHE-SS-biotin. We found that approximately 50% of the WT protein was targeted to the cell surface (Fig. 3B). In contrast, G305R protein was mis-targeted. There was no significant targeting of the protein to the cell surface. As noted above, all of the protein was partially or de-glycosylated, which we have earlier found is characteristic of mis-targeted NHE1 proteins (13,14).

To illustrate the targeting of the WT and mutant NHE1 within the cells, we used immunocytochemistry. Figure 3C illustrates two examples each of the localization of NHE1 in the two cell types. WT (upper panels) showed strong plasma membrane localization. In contrast, cells containing the G305R mutant (lower panels) showed only an intracellular localization of NHE1, which was punctate and at least partially perinuclear. There was no evident plasma membrane localization.

We then used a fluorometric assay to determine the activity of the NHE1 mutant G305R protein relative to that of the WT NHE1 protein. Figure 3D illustrates examples of NHE1 activity of a stable cell line expressing either WT, or the G305R mutant protein. Figure 3E shows a summary of the results. The G305R protein had only a tiny fraction (2%) of the WT NHE1 activity that was only slightly greater than the background shown by untransfected AP-1 cells. In contrast the WT, NHE1 protein showed the typically high NHE1 activity that we have noted earlier (13,14).

DISCUSSION

In this study, we report the first identification of a gene involved in Lichtenstein–Knorr syndrome by the demonstration of a loss-of-function missense mutation in *SLC9A1* that segregates with progressive ataxia and deafness in a large consanguineous family. *SLC9A1* was first cloned in 1989 (15) and codes for NHE1, an 815 amino acid protein containing a hydrophobic N-terminal membrane domain of 500 amino acids responsible for Na^+/H^+ exchange transport and a hydrophilic, intracellular 315 amino acid long C-terminus that regulates transport (16). NHE1 is a ubiquitous protein located at the surface of mammalian cells within the plasma membrane. It transports one Na^+ into the cell in exchange for one H^+ against its electrochemical gradient (17). Despite the fact that NHE1 is ubiquitously expressed, evidence that NHE1 function is prominently important for the CNS came from studies of spontaneous and knockout mice models which present with a neurological syndrome including ataxia and epilepsy (10,12). In the spontaneous mouse mutant (*swe*, for slow-wave epilepsy), extensive analysis of all mutant mouse tissues revealed progressive neuronal degeneration only in three regions of the CNS: vestibular nuclei, cochlear nuclei and most prominently deep cerebellar nuclei. These sites of pathology correlate perfectly well with the clinical presentation of the three patients of family C. Despite the fact that the *SLC9A1* mouse models did not present deafness, NHE1 was shown to have an important role in the inner ear by regulating the pH of the endolymphatic sac, which is essential for the normal hearing function. It has been shown that changes in the pH of the endolymphatic sac endolymph causes hearing loss (18). Contrary to the mouse models, which present with severe convulsive seizures and growth retardation, the patients of family C. had no epilepsy. The reason for this is not known at this time. In our analysis of the G305R mutant protein, we found it was almost completely (>90%) mis-targeted and the activity of the mutant protein in AP-1 cells was barely above background levels, at ~2% of the WT protein. It is uncertain at this time if this small amount of activity is real and could account for the milder presentation of the human disease compared with the mouse models, which are a consequence of complete loss-of-function mutations [non-sense mutation p.Lys442* in the *swe* spontaneous model and deletion of three transmembrane domains (amino acids 199–275 of the mouse protein) in the knockout model]. In this respect, the mouse models mimic more closely the Pratap-Chand syndrome that manifests cerebellar atrophy, growth retardation, microcephaly and even epilepsy in 2 of 11 reported children (8), while the patients of family C. present a juvenile Lichtenstein–Knorr syndrome (6,9). Sequencing of the 12 exons of *SLC9A1* in

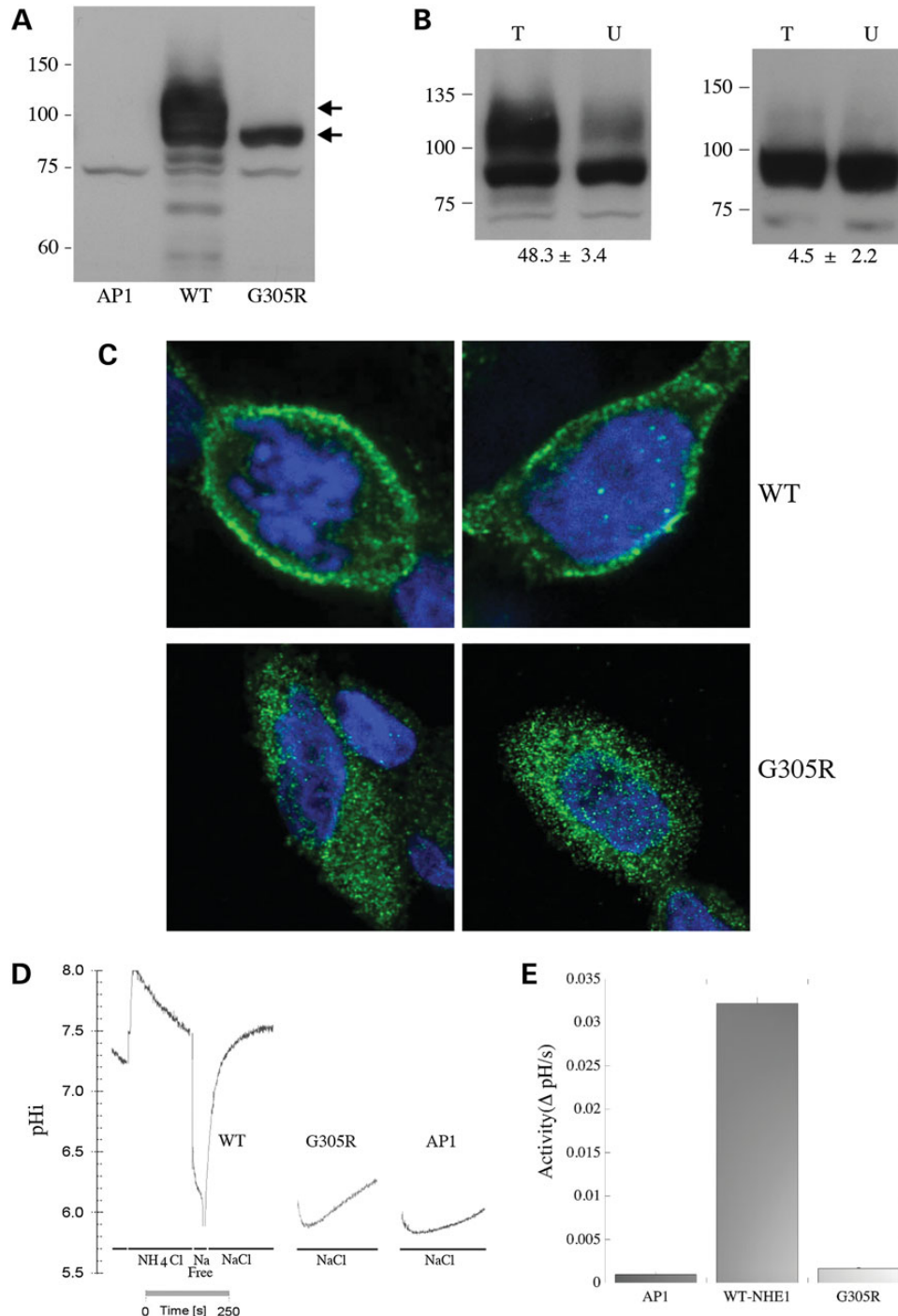


Figure 3. Analysis of WT NHE1 and mutant (G305R) protein. **(A)** Western blot of whole cell lysates of stable cell lines expressing WT Na^+/H^+ exchanger or G305R mutant. The samples were immunoblotted with anti-HA tag antibody. The arrows indicate the position of full length glycosylated NHE1 protein (upper arrow) and partial, or de-glycosylated protein (lower arrow). AP-1 is a cell lysate from mock transfected AP-1 cells. **(B)** Surface targeting of NHE1 in AP-1 cells expressing WT and G305R mutant. Equal amounts of total (T) cell lysate and unbound (U) intracellular lysate were examined by western blotting with anti-HA antibody as described in 'Materials and Methods'. WT and G305R are cell lines stably expressing WT NHE1 and mutant NHE1, respectively. The percent of total NHE1 protein found on the plasma membrane is indicated. Results are the mean \pm SE. $n =$ at least four determinations. **(C)** Immunocytochemical localization of WT and G305R NHE1 proteins in AP-1 cells. Stably transfected cells were prepared for immunocytochemical analysis using anti-HA antibody as described in 'Materials and Methods'. Upper panels, WT NHE1; lower panels, G305R mutant. Green, anti-NHE1 (HA-tag); blue, DAPI (nucleic acid) staining. **(D)** Example of Na^+/H^+ exchanger activity of cell lines containing WT NHE1, G305R NHE1 mutant protein and AP-1 parental cells. NHE1 protein activity was assayed in stably transfected AP-1 cells as described in 'Materials and Methods'. For ease of viewing, only the recovery from acidosis is shown for the G305R protein and AP-1 cells. NH_4Cl , indicates treatment with ammonium chloride. After NH_4Cl treatment, there was a brief 'Na free' treatment to induce acidosis. NaCl, indicates recovery from acidosis in NaCl containing buffer. The acid treatment and entire recovery period are shown for illustrative purposes only. **(E)** Summary of the initial rate of change in intracellular pH mediated by NHE activity in stably transfected AP-1 cells containing WT and mutant (G305R) NHE1 proteins. Activity was measured after ammonium chloride prepulse from the first 20 s of recovery from acidification as described earlier (13) and as described in 'Materials and Methods'. Results are intracellular $\Delta\text{pH/s}$ ($n > 6$).

172 patients with ataxia or deafness revealed no disease-causing variant, suggesting that alteration of NHE1 might only be associated with syndromic ataxia–deafness. Further studies of *SLC9A1* in ataxia/deafness patients are warranted in order to uncover the full spectrum of this unique disorder.

MATERIALS AND METHODS

Ethics statement

Written informed consents, as defined by the Nancy University Hospital Ethics Committee, were obtained prior to blood sampling of members of family C.

Genetic studies

DNA was extracted by standard procedures.

Patients from family C. were analyzed with Affymetrix 50 K Xba 240 SNP arrays according to the protocol provided by the manufacturer (Gene Chip Mapping 100 K Assay manual, Affymetrix, Inc., Santa Clara, CA, USA). Homozygous regions shared between the patients were identified with the HomoSNP software (<http://bips.u-strasbg.fr/HomoSNP/>) that was set to identify regions of 35 or more consecutive homozygous SNPs across the 22 autosomes. In order to demonstrate identity by descent, as opposed to identity by state, SNPs of the shared homozygous regions were then individually inspected to verify that the same haplotype was shared between the patients and that, apart from recombination events, genotypes were identical beyond the homozygous regions.

Whole-exome sequencing was performed by exon capture with the Agilent SureSelect kit and high-throughput sequencing with an Illumina HiSeq2500 sequencer (IGBMC sequencing platform). Approximately 91 million reads were obtained and mapped to the human reference genome (hg19). The median depth of reads over exons was 61.0, with 89.5% of total exons covered by 10 reads or more. Exon coverage with at least one sequence was 95.9%. dbSNP 137 served as a reference to exclude SNPs with a frequency of 1% or above. An additional search in 1000 Genome project and exome variant server (NHLBI GO Exome Sequencing Project) SNP databases was performed to assess the frequency of the selected variants (19). Variants were also analyzed for pathogenicity with in-house pipelines, which combine splice site prediction and protein-coding changes (19).

A search for mutations in patients from family C. was performed examining genes known to be responsible for neurological phenotype including recessive cerebellar ataxia and no mutations were found.

Genomic DNA of 157 patients (156 families) with sporadic or recessive ataxia, 11 patients (8 families with hearing loss), 3 patients (1 family) with sensorineural hearing loss and vestibular dysfunction, and 1 patient with sensorineural hearing loss, retinitis pigmentosa and hypotonia was screened by direct sequencing of the protein-coding exons of *SLC9A1* (12 coding exons).

Functional studies

Materials

2',7-Bis (2-carboxyethyl)-5(6) carboxyfluorescein acetoxy-methyl ester (BCECF-AM) was purchased from Molecular

Probes, Inc. (Eugene, OR, USA). Sulfo-NHS-SS-biotin was purchased from Pierce and synthetic DNA was from IDT (Coralville, IA, USA). All other chemicals that were used were of analytical grade and were purchased from Fisher Scientific (Ottawa, ON, Canada), Sigma (St Louis, MO, USA) or BDH (Toronto, ON, Canada). The plasmid pYN4+ is an expression plasmid containing cDNA for the human NHE1 protein with an HA tag and has been described earlier (20).

Cell culture and stable transfection

To characterize the activity of the mutant versus WT Na⁺/H⁺ exchanger, we used AP-1 cells that are a mutant cell line derived from Chinese hamster ovarian cells that does not express endogenous NHE1 (15). Stably transfected cells were made using LIPOFECTAMINE™ 2000 Reagent (Invitrogen Life Technologies, Carlsbad, CA, USA) as described earlier (13). The NHE1 expression plasmid, pYN4+, has a neomycin resistance gene that allows selection of stably transfected cells using geneticin (G418). Cell lines were regularly re-established from frozen stocks at passage numbers between 5 and 11. The results are typical of at least two stable cell lines.

Cell surface expression

Targeting of the NHE1 protein to the cell surface was measured as described earlier (21). Briefly, the cell surface proteins were labeled with sulfo-NHS-SS-biotin and after solubilization the cell surface Na⁺/H⁺ exchanger was removed with immobilized streptavidin resin. Equivalent amounts of unbound and total protein were separated by sodium dodecyl sulfate polyacrylamide gel electrophoresis (SDS–PAGE) examined by western blotting for immunoreactive (HA-tagged) NHE1 protein. Protein levels on western blots were estimated using the Image J 1.35 software (National Institutes of Health, Bethesda, MD, USA). It was not possible to efficiently and reproducibly elute proteins bound to immobilized streptavidin resin. Amounts of NHE1 on the plasma membrane were estimated by comparing both the upper and lower HA-immunoreactive species.

Immunocytochemistry

AP-1 cells stably expressing WT-NHE1 or G305R mutant were maintained at 37°C, 5% CO₂ and 95% humidity in adherent culture in alpha-minimal essential medium supplemented with 10% bovine growth serum, 12.5 mM HEPES and 400 µg/ml G418. Immunostaining was performed as described earlier (21). Briefly, cells were immunostained with mouse monoclonal anti-HA antibody (1 : 300) to detect HA-tagged NHE1 or G305R mutant. The secondary antibody was Alexa Fluor 488-conjugated goat anti-mouse IgG immunoglobulin (1 : 300 in 0.1% triton-X 100 and 0.1% bovine serum albumin in phosphate buffered saline; Molecular Probes, Eugene, OR, USA). Finally, the cells were washed three times with PBS, and coverslips were mounted using Vectasheild (Vector Laboratories, Burlingame, CA, USA) mounting media containing 4',6-diamidino-2-phenylindole (DAPI). Alexa 488 was excited at 488 nm and detected at 510–560 nm. DAPI was excited with a UV laser and detected at 435–465 nm. Images were taken with a confocal laser scanning microscope (Leica TCS SP5).

SDS–PAGE and immunoblotting

Expression of NHE1 in stable cell lines was confirmed by immunoblotting using antibodies against the HA tag. Samples

were run on 10% SDS–PAGE gels and were transferred to nitrocellulose membranes. The primary antibody was anti-HA monoclonal antibody followed by peroxidase-conjugated goat anti-mouse antibody (Bio/Can, Mississauga, Canada) for signal detection. Reactive protein was detected on X-ray film using the Amersham enhanced chemiluminescence western blotting and detection system.

Intracellular pH measurement

To measure the activity of the Na^+/H^+ exchanger and intracellular pH (pH_i), the fluorescent compound BCECF was used to quantify recovery after an acute acid load was induced as described earlier (13). Cells were grown to approximately 90% confluence on coverslips and fluorescence was quantified using a PTI Deltascan spectrofluorometer. Briefly, acute acidosis was induced with addition and removal of ammonium chloride (50 mm \times 3 min). The first 20 s of recovery from acidification was measured and is expressed as $\Delta\text{pH}/\text{s}$. Calibration of intracellular pH fluorescence was done for each sample (13). Results are the mean \pm standard error (SE) of at least six experiments.

WEB RESOURCES

UCSC Genome Browser: <http://genome.ucsc.edu/index.html>
 Ensembl Genome Browser: <http://www.ensembl.org/index.html> (September 2014)
 Exome Variant Server (EVS), NHLBI GO Exome Sequencing Project (ESP), Seattle, WA: <http://evs.gs.washington.edu/EVS/> (September 2014)
 Human Splicing Finder version 2.4.1: <http://www.umd.be/HSF/> (September 2014)

ACKNOWLEDGEMENTS

We wish to acknowledge the help of Florence Beltramo and Michel Vidailhet for contributions to clinical analysis and of Bernard Jost, Serge Vicaire, Stéphanie Legras, Michael Dumas, Véronique Prigent and Jean Müller for next-generation sequencing and analysis.

Conflict of Interest statement. None declared.

FUNDING

This study was supported by funds from the Institut National de la Santé et de la Recherche Médicale (INSERM), the Agence Nationale pour la Recherche–Maladies Rares et Maladies Neurologiques et Psychiatriques (ANR-09-MNPS-001-01 to M.K.), the ANR/E-rare JTC 2011 ‘Euro-SCAR’ (2011-RARE-004-01 to M.K.). Research by L.F. and X.L. was supported by the Canadian Institute of Health Research.

REFERENCES

- Anheim, M., Tranchant, C. and Koenig, M. (2012) The autosomal recessive cerebellar ataxias. *N. Engl. J. Med.*, **366**, 636–646.
- Fiskerstrand, T., H'mida-Ben Brahim, D., Johansson, S., M'zahem, A., Haukanes, B.I., Drouot, N., Zimmermann, J., Cole, A.J., Vedeler, C.,

- Bredrup, C. *et al.* (2010) Mutations in ABHD12 cause the neurodegenerative disease PHARC: an inborn error of endocannabinoid metabolism. *Am. J. Hum. Genet.*, **87**, 410–417.
- Dürr, A., Cossee, M., Agid, Y., Campuzano, V., Mignard, C., Penet, C., Mandel, J.L., Brice, A. and Koenig, M. (1996) Clinical and genetic abnormalities in patients with Friedreich's ataxia. *N. Engl. J. Med.*, **335**, 1169–1175.
- Hakonen, A.H., Heiskanen, S., Juvonen, V., Lappalainen, I., Luoma, P.T., Rantamaki, M., Goethem, G.V., Lofgren, A., Hackman, P., Paetau, A. *et al.* (2005) Mitochondrial DNA polymerase W748S mutation: a common cause of autosomal recessive ataxia with ancient European origin. *Am. J. Hum. Genet.*, **77**, 430–441.
- Striano, S., Barbieri, F., Meo, R., Bilo, L. and Cirillo, S. (1989) Hearing loss associated with progressive ataxia (Lichtenstein-Knorr disease?). Report of a sporadic case with peculiar neuroradiological findings. *Acta Neurol. (Napoli)*, **11**, 351–359.
- Barbieri, F., De Michele, G., Filla, A., Mansi, D., Santangelo, R., Cirillo, S. and Santoro, L. (1986) Clinical and CT-scan study of a case of cerebellar ataxia and progressive hearing loss: Lichtenstein-Knorr disease? *Acta Neurol. (Napoli)*, **8**, 159–163.
- Heras Pérez, J.A., Asencio Marchante, J.J., Ribas Pérez, C., Juan-Togores Veguero, J.M. and Portillo Balaguer-Cortés, M.F. (1986) [Hereditary ataxia and deafness (Lichtenstein-Knorr disease): study of a family through 5 generations]. *Med. Clin. (Barc.)*, **87**, 508–509.
- Pratap-Chand, R., Gururaj, A.K. and Dilip-Kumar, S. (1995) A syndrome of olivopontocerebellar atrophy and deafness with onset in infancy. *Acta Neurol. Scand.*, **91**, 133–136.
- Lichtenstein, H. and Knorr, A. (1930) Über einige Fälle von fortschreitender Schwerhörigkeit bei hereditärer Ataxie. *Dtsch. Zeitung für Nervenheilkd.*, **114**, 1–28.
- Cox, G.A., Lutz, C.M., Yang, C.L., Biemesderfer, D., Bronson, R.T., Fu, A., Aronson, P.S., Noebels, J.L. and Frankel, W.N. (1997) Sodium/hydrogen exchanger gene defect in slow-wave epilepsy mutant mice. *Cell*, **91**, 139–148.
- Desmet, F.-O., Hamroun, D., Lalande, M., Collod-Bérout, G., Claustres, M. and Bérout, C. (2009) Human Splicing Finder: an online bioinformatics tool to predict splicing signals. *Nucleic Acids Res.*, **37**, e67.
- Bell, S.M., Schreiner, C.M., Schultheis, P.J., Miller, M.L., Evans, R.L., Vorhees, C.V., Shull, G.E. and Scott, W.J. (1999) Targeted disruption of the murine Nhe1 locus induces ataxia, growth retardation, and seizures. *Am. J. Physiol.*, **276**, C788–C795.
- Slepkov, E.R., Rainey, J.K., Li, X., Liu, Y., Cheng, F.J., Lindhout, D.A., Sykes, B.D. and Fliegel, L. (2005) Structural and functional characterization of transmembrane segment IV of the NHE1 isoform of the Na^+/H^+ exchanger. *J. Biol. Chem.*, **280**, 17863–17872.
- Ding, J., Rainey, J.K., Xu, C., Sykes, B.D. and Fliegel, L. (2006) Structural and functional characterization of transmembrane segment VII of the Na^+/H^+ exchanger isoform 1. *J. Biol. Chem.*, **281**, 29817–29829.
- Sardet, C., Franchi, A. and Pouyssegur, J. (1989) Molecular cloning, primary structure, and expression of the human growth factor-activatable Na^+/H^+ antiporter. *Cell*, **56**, 271–280.
- Wakabayashi, S., Pang, T., Su, X. and Shigekawa, M. (2000) A novel topology model of the human $\text{Na}^+(\text{+})/\text{H}^+(\text{+})$ exchanger isoform 1. *J. Biol. Chem.*, **275**, 7942–7949.
- Franchi, A., Perucca-Lostanlen, D. and Pouyssegur, J. (1986) Functional expression of a human Na^+/H^+ antiporter gene transfected into antiporter-deficient mouse L cells. *Proc. Natl. Acad. Sci. USA*, **83**, 9388–9392.
- Son, E.J., Moon, I.S., Kim, S.H., Kim, S.J. and Choi, J.Y. (2009) Interferon-gamma suppresses Na^+/H^+ exchanger in cultured human endolymphatic sac epithelial cells. *J. Cell. Biochem.*, **107**, 965–972.
- DePristo, M.A., Banks, E., Poplin, R., Garimella, K.V., Maguire, J.R., Hartl, C., Philippakis, A.A., del Angel, G., Rivas, M.A., Hanna, M. *et al.* (2011) A framework for variation discovery and genotyping using next-generation DNA sequencing data. *Nat. Genet.*, **43**, 491–498.
- Li, X., Ding, J., Liu, Y., Brix, B.J. and Fliegel, L. (2004) Functional analysis of acidic amino acids in the cytosolic tail of the Na^+/H^+ exchanger. *Biochemistry*, **43**, 16477–16486.
- Slepkov, E.R., Chow, S., Lemieux, M.J. and Fliegel, L. (2004) Proline residues in transmembrane segment IV are critical for activity, expression and targeting of the Na^+/H^+ exchanger isoform 1. *Biochem. J.*, **379**, 31–38.